DOI: 10.1021/ma101862b

Macromolecules
ARTICLE

Amperometric Detection of Glucose Using a Conjugated Polyelectrolyte Complex with Single-Walled Carbon Nanotubes

Xin Pang,[†] Patigul Imin,[†] Igor Zhitomirsky,*[,‡] and Alex Adronov*[,†]

[†]*Department of Chemistry and Chemical Biology and* [‡]*Department of Materials Science and Engineering, McMaster University, Hamilton, Ontario, Canada*

Received August 13, 2010; Revised Manuscript Received November 15, 2010

ABSTRACT: The conjugated polymer, poly[3-(3-*N*,*N*-diethylaminopropoxy)thiophene] (PDAOT), was synthesized and employed in the supramolecular functionalization of single-walled carbon nanotubes (SWNTs). Highly stable aqueous solutions of PDAOT−SWNT complexes were obtained after sonication under mildly acidic conditions. UV−vis absorption and Raman spectroscopy studies showed that the noncovalent functionalization did not change the nanotube structure and retained its inherent properties. The reactions of $[Fe(CN_6)]^{3-/4-}$ redox couple on Au electrodes modified with PDAOT and the PDAOT−SWNT films were studied using electrochemical impedance spectroscopy and cyclic voltammetry. A lower electron-transfer resistance and higher current response were observed on the Au/PDAOT−SWNT electrode compared with the Au/PDAOT electrode. We prepared glucose biosensors by entrapping glucose oxidase (GOx) within the PDAOT and PDAOT−SWNT films. Under optimized conditions, the Au/PDAOT−SWNT/GOx biosensor exhibited fast current response to glucose with a detection limit of 5 μM and a sensitivity of 700 ± 26 $\mu A/mM \cdot cm^2$. The responsiveness of the Au/PDAOT−SWNT/GOx biosensor can be attributed to the synergistic effect of the high conductivity and nondenaturing microenvironment of the PDAOT and the large active surface area and electrical conductivity provided by the SWNTs.

Introduction

To take full advantage of the unique properties of carbon nanotubes (CNTs) in practical applications, control over their dispersion and physical characteristics must be achieved.[1−4] In particular, the preparation of CNT-rich coatings, patterns, and deposits requires nanotube solutions in various organic and aqueous solvents. However, the inherent insolubility of both multiwalled and single-walled CNTs (MWNTs and SWNTs, respectively)[5] has posed a significant challenge to their solution-phase manipulation. Fortunately, it has recently been shown that both covalent and noncovalent chemical functionalization of CNTs enables their dissolution in a wide variety of solvents.[5−9] In particular, supramolecular functionalization has attracted significant attention because this strategy enables dissolution of CNTs without disrupting any of their original strength and conductivity properties.[10] To this end, the wrapping of CNTs with conjugated polymers (CPs) has been investigated in recent literature as a result of the high affinity of this class of polymers for the nanotube surface.[11−19] In addition, a variety of properties can be introduced into the resulting supramolecular complexes through manipulation of the polymer backbone and side chains.[20,21] Recent examples include tightly binding CNT complexes with poly(thiophene) and poly(fluorene) derivatives that are not only soluble in organic and aqueous solvents but also can enable high-resolution surface patterning, electrophoretic deposition, and separation of nanotubes according to type.[22−25] The high degree of solubility achievable with this approach provides an opportunity to apply homogeneously dispersed CNTs within a variety of device constructs that take advantage of the unique nanotube conductivity properties, including field effect transistors, photovoltaics, light-emitting diodes, and sensors.

*Corresponding authors. (A.A.) E-mail: adronov@mcmaster.ca. Tel: (905) 525-9140, ext. 23514. Fax: (905) 521-2773. (I.Z.) E-mail: zhitom@mcmaster.ca. Tel: (905) 525-9140, ext. 23914. Fax: (905) 528-9295.

In the general area of electrochemical biosensors, the use of CPs as signal mediators has become widespread because of their remarkable stability, processability, solubility, electrical conductivity, and compatibility with biomolecules in aqueous solutions.[26−29] In addition to providing a suitable immobilization matrix for enzymes, antibodies, and nucleic acids, CPs have the potential to enhance stability and sensitivity of biosensors.[30−33] Poly(thiophene), along with its derivatives, represents a versatile class of CPs especially amenable for sensor applications, on account of their interesting optical and electronic properties[34] as well as the facile ability to modify their structure with various side-chain functionalities that enable binding to enzymes, mediators, and compatibilizing groups.[35] A more important advantage of poly(thiophene) over other conducting polymers as immobilization matrix in amperometric enzyme electrodes is its excellent stability in both air and water, making it relatively resistant to degradation by enzymatically generated oxidants, such as H_2O_2.[36]

Recently, improvements upon the CP biosensors have been realized through incorporation of nanostructures such as metal nanoparticles[37] and CNTs.[38,39] In the case of CNTs, the high mobility of charge carriers in semiconducting tubes coupled to their large surface area makes them ideal candidates for sensor applications.[40] Additionally, as mentioned above, wrapping of nanotubes with CPs not only improves their solubility and general processability but also combines two materials having useful electrochemical properties. However, to date, nanotube complexes with only a limited variety of CPs have been investigated in glucose biosensor applications, including Nafion,[41,42] electropolymerized poly(pyrrole),[43,44] and in situ prepared poly(aniline).[45] Although encouraging results have been reported with these systems, it is reasonable to assume that the CP−nanotube−biomolecule interactions can be optimized by varying the CP structure and properties. It is also advantageous to expand this CP repertoire to polymers that can easily be prepared, modified, and characterized prior to incorporation into biosensors.

 Published on Web 12/02/2010

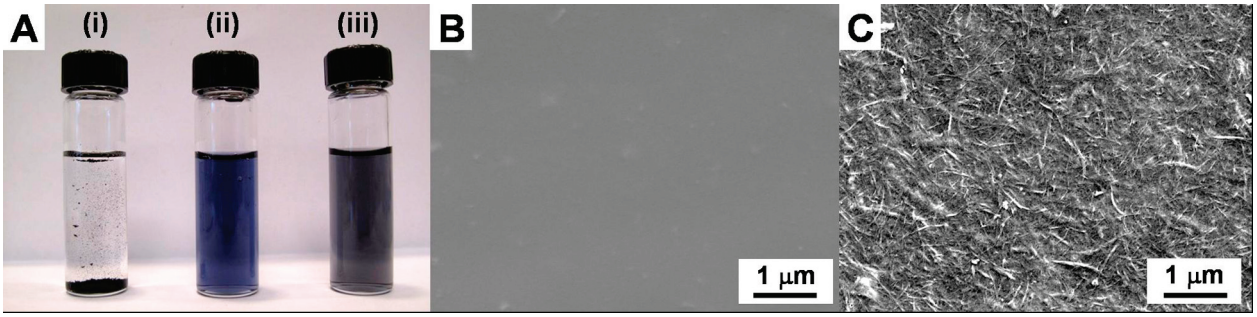

Figure 1. (A) Photograph of vials containing (i) pristine SWNTs, (ii) PDAOT, and (iii) PDAOT−SWNT complexes in water after sonication for 1 h; (B) SEM image of a drop-cast film prepared from a 6 g/L aqueous solution of PDAOT; (C) SEM image of a drop-cast film prepared from an aqueous mixture of 6 g/L PDAOT and 6 g/L SWNTs.

Scheme 1. Procedure for Synthesis of Poly[3-(3-*N*,*N*-diethylaminopropoxy)thiophene] (PDAOT)

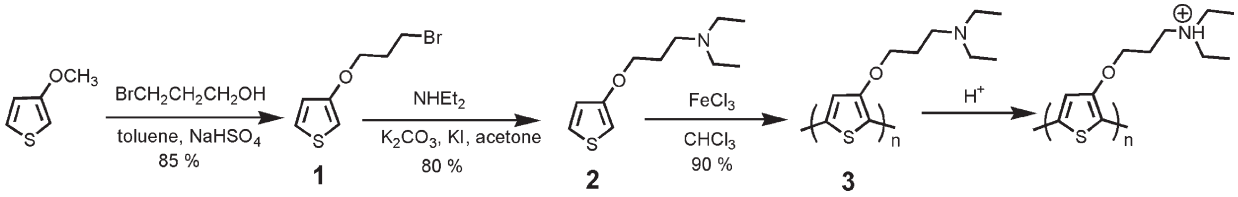

In this investigation, a poly(thiophene) derivative, poly[3-(3-*N*,*N*-diethylaminopropoxy)thiophene] (PDAOT), was prepared through oxidative solution polymerization and utilized for the supramolecular functionalization of SWNTs, resulting in highly stable and concentrated aqueous solutions of PDAOT−SWNT complexes. The addition of glucose oxidase (GOx) to these solutions, followed by deposition onto gold electrodes, resulted in PDAOT−SWNT loaded polymer layers that contained entrapped GOx and formed highly sensitive glucose biosensors. The results presented here show that the PDAOT−SWNT complexes offer a versatile platform for the immobilization of enzymes within coatings that exhibit fast electron-transfer kinetics, high electrical conductivity, and excellent film quality. The obtained results pave the way for the development of other advanced biosensors based on SWNTs.

Results and Discussion

Synthesis of Conjugated Polymer PDAOT. The poly(thiophene) derivative PDAOT was prepared by oxidative polymerization of the 3-(3-*N*,*N*-diethylaminopropoxy)thiophene monomer, as depicted in Scheme 1. 3-(3-Bromo)propoxythiophene **1** was prepared by treatment of 3-methoxythiophene with 2-bromo-1-propanol in the presence of $NaHSO_4$, as previously reported.[46] Subsequent treatment of **1** with diethylamine produced the amine-functionalized thiophene monomer **2**. PDAOT polymer **3** was then prepared under oxidative polymerization conditions in chloroform using ferric chloride as the oxidant. The neutral PDAOT (**3**) is readily soluble in common organic solvents such as chloroform and THF but insoluble in water and low-boiling alcohols (methanol and ethanol). Protonation of the amine side-chains with small amounts of acetic acid (5% vol/vol) resulted in complete and rapid dissolution of the polymer in water or ethanol, forming a blue solution (Figure 1A, ii).

Investigation of the PDAOT−SWNT Supramolecular Interaction. The supramolecular functionalization of SWNTs by PDAOT was accomplished by previously published procedures[23] (Supporting Information) and resulted in a homogeneous solution of PDAOT−SWNT complexes that was stable for several weeks without nanotube precipitation (Figure 1A, iii). The control experiment using pristine SWNTs treated identically but in the absence of PDAOT did not exhibit any observable solubility (Figure 1A, i). The scanning electron microscopy (SEM) images in Figure 1B,C show the surface of drop-cast films of PDAOT and PDAOT−SWNT complexes. A relatively smooth and dense polymer film was formed after evaporation of the solvent (i.e., water), owing to the excellent film formation properties of PDAOT (Figure 1B). When mixed with SWNTs, the strong supramolecular interactions between PDAOT and the nanotubes resulted in significant debundling and homogeneous dispersion of SWNTs in the polymer matrix, leading to the formation of a composite film of PDAOT−SWNT complexes upon solvent evaporation (Figure 1C).

The PDAOT−SWNT supramolecular interactions were studied by Raman and UV−vis spectroscopy. Figure 2A provides the Raman spectra of pristine SWNTs and dropcast films of PDAOT alone and the PDAOT−SWNT complexes on glass slides. The spectra for samples containing SWNTs were normalized to the graphitic (G) band at 1590 cm^{-1}. The Raman bands of PDAOT (Figure 2A, curve a) match the experimental and calculated major Raman bands of poly(alkoxy thiophene)s reported in the literature.[47,48] The Raman spectrum of the PDAOT−SWNT complexes (Figure 2A, curve c) exhibits characteristic features of both the SWNTs and polymer components. The G band position (~1590 cm^{-1}) for the PDAOT−SWNT complexes did not shift compared with that of the pristine nanotubes (Figure 2A, curve b). In addition, no significant increase in the intensity of the disorder (D) band at ~1300 cm^{-1} was observed for the PDAOT−SWNT complexes compared with the pristine SWNTs, indicating that the supramolecular functionalization did not introduce any defects or structural changes into the SWNT sidewall. The radial breathing mode (RBM) profiles can be clearly observed in the Raman spectra for the pristine SWNTs and the dropcast PDAOT−SWNT film. The decrease in intensity and small shifts of peak positions of various RBM signals after the supramolecular functionalization may be attributed to electronic interactions between PDAOT and SWNTs.

UV−vis spectroscopy was also performed to study the PDAOT−SWNT superamolecular interactions and the possible conformational change of GOx after it was immobilized with PDAOT and the PDAOT−SWNT complexes. The spectrum of

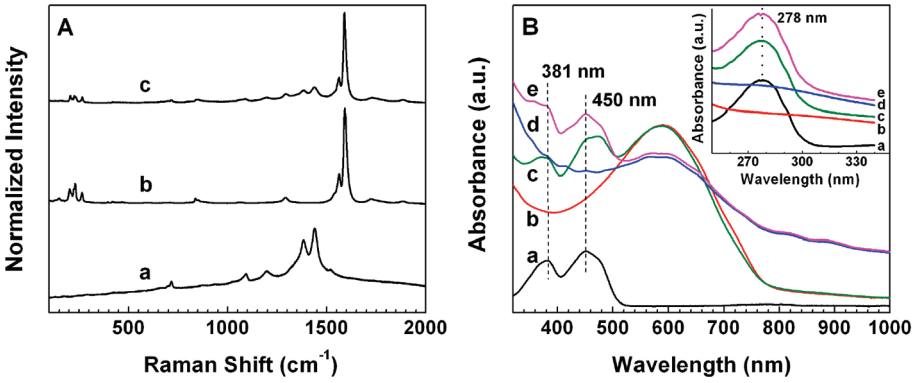

Figure 2. (A) Raman spectra for (a) PDAOT, (b) pristine SWNTs, and (c) PDAOT−SWNT complexes. (B) UV−vis absorption data for aqueous solutions containing (a) GOx, (b) PDAOT, (c) PDAOT and GOx, (d) PDAOT−SWNT complexes, and (e) PDAOT−SWNT complexes with 2 g/L GOx added. Inset: Absorption data in the short wavelength region for samples a−e after two-fold dilution.

PDAOT−SWNT complexes (Figure 2B, curve d) revealed absorption bands corresponding to both the polymer (Figure 2B, curve b) at 589 nm and the SWNTs (weak van Hove singularities at 700−900 nm, along with a steady increase in absorption at shorter wavelengths). There was no shift in the absorption maximum of PDAOT upon nanotube complexation, indicating that PDAOT must adopt a relatively planar conformation in solution, and the degree of planarity (along with conjugation length) does not change appreciably upon adsorption to the SWNT surface. Figure 2B (curve a) shows the UV−vis absorption spectrum of the enzyme GOx, with its characteristic absorption peaks at 278, 381, and 450 nm.[49−52] The absorption band at 278 nm is assigned to the characteristic peak of the polypeptide chains in the GOx structure,[51,52] and the peaks at 381 and 450 nm are characteristic of the oxidized form of the flavin group.[49,50] The spectrum of PDAOT/GOx (Figure 2B, curve c) exhibited both absorption bands corresponding to the polymer at 589 nm and the GOx (at 278, 382, and 473 nm). The spectrum of PDAOT−SWNT/GOx (Figure 2B, curve e) showed three additional absorption bands compared with that of PDAOT−SWNT complexes, whose position and peak shape are the same as those for pure GOx. In addition, the absorption of GOx did not change to any extent when the PDAOT−SWNT/GOx mixture was cast as a solid film on a quartz substrate. (See Figure S1 of the Supporting Information.) These results suggest that the GOx immobilized with the PDAOT and the PDAOT−SWNT complexes retains its native structure and therefore should maintain its bioactivity. The chromophoric GOx flavin groups remain embedded in the GOx polypeptide matrix and do not unfold from their hydrophobic interior domains upon immobilization.[51,52]

To corroborate these results further, circular dichroism (CD) measurements were performed on the native GOx, the PDAOT/GOx mixture, and the PDAOT−SWNT/GOx material, which was redissolved from the surface of the electrode after dropcasting on the electrode surface. The CD spectrum of GOx in its native state exhibits strong CD signals in the visible, near-UV, and far-UV regions (Figure 3).[53] These include strong positive absorptions at ca. 380 and 270 nm from the flavin moiety and the aromatic tryptophans in the active site, respectively. The strong negative signal in the far-UV region, centered around 210 nm, results from n→π^* transitions that are sensitive to the secondary structure of GOx. Comparison of the native GOx with the material that has been mixed with polymer and polymer-nanotube complexes indicates no change in the CD spectrum upon exposure to the electrode coating components, again confirming that the enzyme retains its native form even after casting within an active coating on the electrode surface.

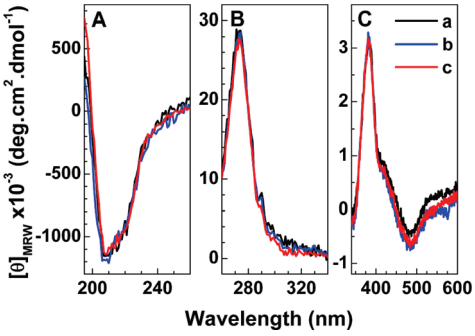

Figure 3. Circular dichroism of (a) GOx, (b) GOx and PDAOT, and (c) a mixture of GOx, PDAOT, and SWNT in the (A) far-UV region, (B) near-UV region, and (C) visible region. The GOx concentration was (A) 0.05, (B) 5, and (C) 20 g/L in a 1 mm cuvette.

Electrochemical Characterization of Modified Electrodes. Electrochemical impedance spectroscopy (EIS) is a highly effective method for probing the features of the surface of modified electrodes.[54,55] EIS was therefore carried out to investigate the electron-transfer properties of the PDAOT and PDAOT−SWNT coatings. Figure 4A shows typical impedance spectra, in the form of Nyquist plots, acquired from the Au electrodes modified with films of pure polymer (Figure 4A, curve a) and PDAOT−SWNT complexes (Figure 4A, curve b). The profiles manifested a very small semicircular domain at high frequencies corresponding to the electron-transfer limited process and a straight line at low frequencies that corresponds to the diffusion process. The Randles equivalent circuit (inset of Figure 4A)[56−58] was chosen to fit the impedance data obtained, where R_s is the solution resistance, R_{et} is the electron-transfer resistance, W is the Warburg impedance, and C_{dl} is the double-layer capacitance. From these data, it was determined that the Au/PDAOT electrode (Figure 4A, curve a) exhibited a small electron-transfer resistance (R_{et}) corresponding to 2.9 $\Omega \cdot cm^2$, which was calculated from the radius of the semicircular domain of the Nyquist plot. The R_{et} value may be ascribed to the conductivity of the CP. The Au/PDAOT−SWNT electrode (Figure 4A, curve b) showed a lower R_{et} (0.8 $\Omega \cdot cm^2$), indicating that the presence of SWNTs enhanced the electron transfer from the redox probe.

Cyclic voltammetry of the ferricyanide/ferrocyanide system has also been conducted to study further the enhanced electrochemical response of the Au/PDAOT−SWNT electrode. Figure 4B shows cyclic voltammograms (CVs) of the Au/PDAOT and Au/PDAOT−SWNT electrodes in 5.0 mM ferricyanide/ferrocyanide solution. Well-defined oxidation and reduction peaks of $[Fe(CN)_6]^{3-/4-}$ were observed with

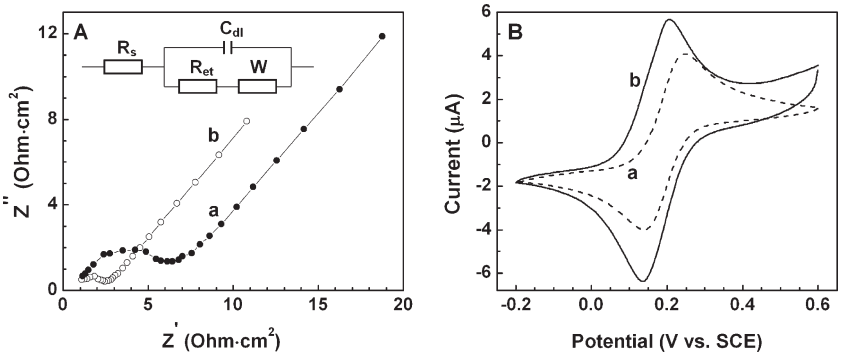

Figure 4. (A) Nyquist plots and the equivalent electrical circuit (inset) of EIS data and (B) CVs for (a) Au/PDAOT and (b) Au/PDAOT−SWNT electrodes prepared using 3 g/L PDAOT aqueous solution and 3 g/L PDAOT aqueous solution containing 1.5 g/L SWNTs, respectively. The electrolyte was a 0.1 mM KCl aqueous solution containing 5 mM $K_3[Fe(CN)_6]/K_4[Fe(CN)_6]$ (1:1). In the equivalent circuit, the R_s is the solution resistance, R_{et} is the electron-transfer resistance, W is the Warburg impedance, and C_{dl} is the double-layer capacitance.

both electrodes. The PDAOT on the electrode surface is positively charged because of protonation, and it adsorbs the negatively charged ferricyanide and ferrocyanide to the electrode, resulting in a high current response. The incorporation of SWNTs into the PDAOT film led to an increase in the oxidation and reduction peak currents of the electrode (Figure 4B, curve b). This can be attributed to the porous microstructure and increased specific surface area of the PDAOT−SWNT film. The peak-to-peak separation (ΔE_p) was 108 and 69 mV for the Au/PDAOT and Au/PDAOT−SWNT electrodes, respectively. A smaller ΔE_p indicates faster electron-transfer kinetics for the Au/PDAOT−SWNT electrode as compared with the Au/PDAOT electrode that lacks the SWNTs.

The CVs are consistent with the EIS data. The enhanced charge transfer at the Au/PDAOT−SWNT electrode is due to the presence of well-dispersed SWNTs in the polymer matrix, which provide a conducting network facilitating charge transport through the film. Furthermore, SWNTs have shown excellent catalytic properties toward the electrochemical processes of many compounds.[41,59−61] Polymer/SWNT composites have been reported to improve electrocatalytic activation of redox enzymes by enhancing electrochemical transduction of the biochemical process.[62] It is expected that the film of PDAOT−SWNT complexes can act as a superior platform for the immobilization of enzymes such as GOx, with enhanced charge transport and bioelectrocatalytic properties, yielding high electrochemical responses.

Optimization of Operation Potential of Biosensors. Glucose biosensors were constructed by modifying Au electrode coatings of PDAOT and PDAOT−SWNT with entrapped GOx. A 6 g/L PDAOT aqueous solution containing 5 g/L GOx and an aqueous mixture of 6 g/L PDAOT and 6 g/L SWNTs containing 5 g/L GOx were used to prepare Au/PDAOT/GOx and Au/PDAOT−SWNT/GOx glucose biosensors, respectively. The operating potential of the biosensors was optimized by amperometric response experiments. Figure 5 shows the current response to glucose as a function of the applied potential in the range from 0.45 to 1.0 V for Au/PDAOT/GOx (Figure 5, curve a) and Au/PDAOT−SWNT/GOx (Figure 5, curve b) biosensors. For Au/PDAOT/GOx, the current response increased with the increasing applied potential to reach a maximum at +0.8 V and then slightly decreased at more positive potentials. For Au/PDAOT−SWNT/GOx (Figure 5b), the maximum current was reached at +0.9 V. The current response increased rapidly with the increase in applied potential when the potential was lower than +0.8 V, indicating that the current

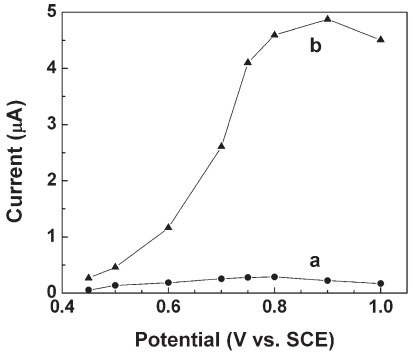

Figure 5. Dependences of the current response to 1 mM glucose for (a) Au/PDAOT/GOx and (b) Au/PDAOT−SWNT/GOx on the applied potential in a 0.1 M phosphate buffered saline (pH 7.4).

response is controlled by the electrochemical oxidation of the enzymatically generated H_2O_2

$$\text{glucose} + O_2 \xrightarrow{GOx} \text{gluconolactone} + H_2O_2$$

$$H_2O_2 \rightarrow O_2 + 2H^+ + 2e^-$$

When the potential was higher than +0.8 V, the current became relatively constant, which resulted from the rate-limiting process of enzyme kinetics.[63,64] In subsequent experiments, a potential of +0.8 V was selected for the operation of the Au/PDAOT/GOx and Au/PDAOT−SWNT/GOx biosensors. EIS data were also measured at the detection potential (+0.8 V) for the Au/PDAOT−SWNT electrode and resulted in a low R_{et} value of 1.1 $\Omega \cdot cm^2$, consistent with the measurement at open circuit potential. (See Figure S2 of the Supporting Information.)

Amperometric Detection of Glucose. Figure 6 shows the current−time plots for the Au/PDAOT/GOx and Au/PDAOT−SWNT/GOx biosensors under the optimized applied potential (+0.8 V) with successive increase in glucose concentration in 0.2 mM increments. Rapid (within < 5 s) response to glucose was observed for both electrodes, but a much higher sensitivity was observed in the presence of SWNTs (Figure 6b) as compared with the Au/PDAOT/GOx electrode (Figure 6a). The Au/PDAOT−SWNT/GOx biosensors exhibited linear current responses to successive increase in glucose over a range of 0.2−5 mM (Figure 6B) with a low detection limit of 5 μM at a signal-to-noise ratio of 3. A current sensitivity of $100 \pm 6.0\,\mu A/mM \cdot cm^2$ was observed for Au/PDAOT/GOx, whereas Au/PDAOT−SWNT/GOx showed a higher sensitivity of 700 ± 26 $\mu A/mM \cdot cm^2$. The sensitivity of the Au/PDAOT−SWNT/GOx

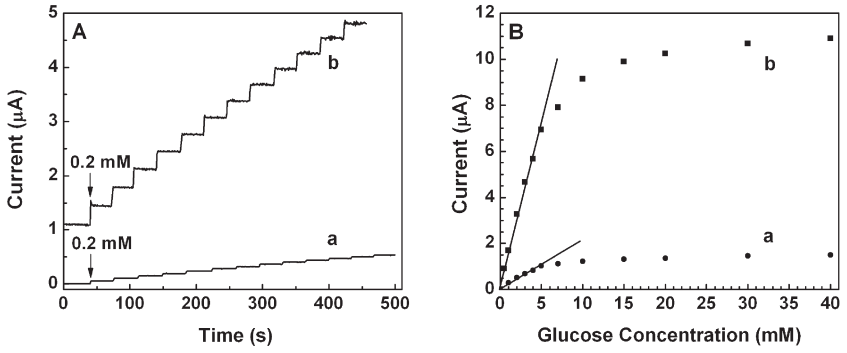

Figure 6. (A) Amperometric responses to successive increase of 0.2 mM glucose in 0.1 M phosphate buffered saline (pH 7.4) at +0.8 V versus SCE and (B) steady-state calibration curves for the (a) Au/PDAOT/GOx and (b) Au/PDAOT−SWNT/GOx electrodes.

biosensor is much higher than what has previously been reported for glucose biosensors constructed using other polymers and CNTs.[42−45] The sensitivity of the Au/PDAOT−SWNT/GOx biosensor is likely the result of the synergistic effect of the high conductivity and enzyme-compatible environment provided by the PDAOT−SWNT complexes, which also act as individual nanoscale electrodes providing a high effective electrode surface area.

When the glucose concentration was high, a plateau of current response was observed, showing the characteristic Michaelis−Menten kinetics for GOx. The apparent Michaelis−Menten constant (K_m^{app}) can be calculated from the electrochemical version of the Lineweaver−Burk equation[65]

$$\frac{1}{i_{ss}} = \left(\frac{K_m^{app}}{i_{max}}\right)\frac{1}{C} + \frac{1}{i_{max}}$$

where i_{ss} is the steady-state current after the addition of substrate, i_{max} is the maximum current under saturated substrate conditions, and C is the concentration of substrate. The K_m^{app} value for the Au/PDAOT−SWNT/GOx biosensor was found to be 3.4 mM, which was much smaller than those of native GOx in solution (33 mM)[49] and immobilized GOx in polyaniline (31.59 mM),[66] polypyrrole (25.3 mM),[67] chitosan (21 mM),[68] and MWCNT/Teflon composite (30 mM).[69] This result reveals that the GOx entrapped in the PDAOT−SWNT composite film exhibits high enzymatic activity and biological affinity to glucose.

Detection Selectivity. Difficulties in accurate measurement of glucose concentration can arise from electroactive interfering compounds such as ascorbic acid (AA), uric acid (UA), and acetaminophen (AP), which are commonly present within physiological samples. We tested the selectivity of the above biosensor design by adding these interfering compounds at the concentrations typically found within blood (0.1, 0.3, and 0.1 mM for AA, UA, and AP, respectively). Unfortunately, in the absence of any modification, the biosensor was highly sensitive to these compounds, giving signals that were on the order of 20−100% of the magnitude observed for glucose at a concentration of 5 mM. However, the introduction of Nafion as an overcoat on the electrode surface dramatically reduced the sensitivity to the interfering compounds while retaining much of the sensitivity to glucose (Figure 7 and Table 1). Under these conditions, interference from UA, AA, and AP amounted to 3.5, 2.3, and 13.9%, respectively, relative to the response upon the introduction of a 5 mM concentration of glucose (Table 1). It should be noted that the second glucose addition in Figure 7 produced a decreased response relative to the first addition because at that point the glucose concentration was beyond the dynamic range for the sensor. Improvement in the selectivity of this biosensor design through variation of sensor components and glucose detection mechanism is the subject of ongoing research.

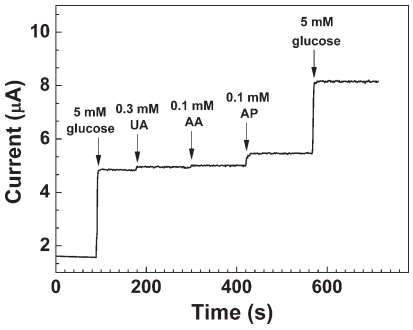

Figure 7. Amperometric response to sequential additions of glucose, AA, UA, and AP.

Table 1. Nafion-Coated Sensor Response to the Addition of Interfering Compounds

analyte[a]	current response (μA)	relative response[b]
5.0 mM glucose	3.30	100%[c]
0.3 mM uric acid	0.116	3.52%
0.1 mM ascorbic acid	0.078	2.36%
0.1 mM acetaminophen	0.460	13.9%
5.0 mM glucose	2.69	81.5%

[a] Analytes were sequentially added in the order shown. [b] Response relative to the initial 5.0 mM glucose addition. [c] Sensitivity to the initial 5.0 mM glucose addition was calculated to be 336.2 $\mu A/mM \cdot cm^2$.

Conclusions

We have demonstrated a promising glucose biosensor by immobilizing GOx within the composite film of PDAOT−SWNT complexes. The water-soluble CP, PDAOT, was synthesized by oxidative polymerization and utilized for the supramolecular functionalization of SWNTs. The PDAOT−SWNT complexes form stable aqueous solutions that can be used for the fabrication of highly sensitive amperometric glucose biosensor. The experimental results showed that Au electrodes modified with a film of PDAOT−SWNT complexes can provide a universal platform for the immobilization of redox enzymes, with excellent electronic conductivity and enhanced electron transfer properties. The incorporation of SWNTs into the polymer matrix increased both the electron transfer rate and the total current flowing through the coating. Under optimized conditions, the Au/PDAOT−SWNT/GOx biosensor exhibited fast current response to glucose with a sensitivity of $700 \pm 26\ \mu A/mM \cdot cm^2$ and a detection limit of 5 μM (S/N = 3). We achieved selectivity of this sensor design by introducing a Nafion overcoat, which effectively suppressed the response to AA, UA, and AP while maintaining much of the sensor sensitivity to glucose. The excellent performance of the biosensor

can be attributed to the synergistic effect of the high conductivity and nondenaturing microenvironment of the PDAOT as well as the large active surface area and electrical conductivity provided by the SWNTs. The results of this investigation pave the way for the fabrication of other redox-enzyme-based biosensors using PDAOT−SWNT complexes.

Acknowledgment. We gratefully acknowledge the financial support of the Natural Sciences and Engineering Research Council of Canada. P.I. gratefully acknowledges the Ontario Ministry of Training for an Ontario Graduate Scholarship.

Supporting Information Available: Experimental procedures are described for the synthesis of the conjugated polymer PDAOT, characterization of the PDAOT−SWNT supramolecular interactions, and the electrochemical testing of the enzyme electrode biosensors prepared using the polymer alone and the PDAOT−SWNT complexes. This material is available free of charge via the Internet at http://pubs.acs.org.

References and Notes

(1) Endo, M.; Strano, M. S.; Ajayan, P. M. *Top. Appl. Phys.* **2008**, *111*, 13–62.
(2) Baughman, R. H.; Zakhidov, A. A.; de Heer, W. A. *Science* **2002**, *297*, 787–792.
(3) Grossiord, N.; Loos, J.; Regev, O.; Koning, C. E. *Chem. Mater.* **2006**, *18*, 1089–1099.
(4) Terrones, M. *Annu. Rev. Mater. Res.* **2003**, *33*, 419–501.
(5) Tasis, D.; Tagmatarchis, N.; Bianco, A.; Prato, M. *Chem. Rev.* **2006**, *106*, 1105–1136.
(6) Banerjee, S.; Hemraj-Benny, T.; Wong, S. S. *Adv. Mater.* **2005**, *17*, 17–29.
(7) Bahr, J. L.; Tour, J. M. *J. Mater. Chem.* **2002**, *12*, 1952–1958.
(8) Bahun, G. J.; Cheng, F.; Homenick, C. M.; Lawson, G.; Zhu, J.; Adronov, A. In *Chemistry of Carbon Nanotubes*; Basiuk, V. A., Basiuk, E. V., Eds.; American Scientific Publishers: Stevenson Ranch, CA, 2008; Vol. *2*, pp 191−242.
(9) Singh, P.; Campidelli, S.; Giordani, S.; Bonifazi, D.; Bianco, A.; Prato, M. *Chem. Soc. Rev.* **2009**, *38*, 2214–2230.
(10) Britz, D.; Khlobystov, A. *Chem. Soc. Rev.* **2006**, *35*, 637–659.
(11) Tang, B. Z.; Xu, H. Y. *Macromolecules* **1999**, *32*, 2569–2576.
(12) Chen, J.; Liu, H. Y.; Weimer, W. A.; Halls, M. D.; Waldeck, D. H.; Walker, G. C. *J. Am. Chem. Soc.* **2002**, *124*, 9034–9035.
(13) Star, A.; Stoddart, J. F.; Steuerman, D.; Diehl, M.; Boukai, A.; Wong, E. W.; Yang, X.; Chung, S. W.; Choi, H.; Heath, J. R. *Angew. Chem., Int. Ed.* **2001**, *40*, 1721–1725.
(14) Steuerman, D. W.; Star, A.; Narizzano, R.; Choi, H.; Ries, R. S.; Nicolini, C.; Stoddart, J. F.; Heath, J. R. *J. Phys. Chem. B* **2002**, *106*, 3124–3130.
(15) Star, A.; Steuerman, D. W.; Heath, J. R.; Stoddart, J. F. *Angew. Chem., Int. Ed.* **2002**, *41*, 2508–2512.
(16) Star, A.; Liu, Y.; Grant, K.; Ridvan, L.; Stoddart, J. F.; Steuerman, D. W.; Diehl, M. R.; Boukai, A.; Heath, J. R. *Macromolecules* **2003**, *36*, 553–560.
(17) Rice, N. A.; Soper, K.; Zhou, N.; Merschrod, E.; Zhao, Y. *Chem. Commun.* **2006**, 4937–4939.
(18) Cheng, F. Y.; Adronov, A. *Chem.—Eur. J.* **2006**, *12*, 5053–5059.
(19) Cheng, F. Y.; Zhang, S.; Adronov, A.; Echegoyen, L.; Diederich, F. *Chem.—Eur. J.* **2006**, *12*, 6062–6070.
(20) Heeger, A. *Chem. Soc. Rev.* **2010**, *39*, 2354–2371.
(21) Beaujuge, P.; Reynolds, J. *Chem. Rev* **2010**, *110*, 268–320.
(22) Cheng, F.; Imin, P.; Lazar, S.; Botton, G. A.; de Silveira, G.; Marinov, O.; Deen, J.; Adronov, A. *Macromolecules* **2008**, *41*, 9869–9874.
(23) Casagrande, T.; Imin, P.; Cheng, F.; Botton, G. A.; Zhitomirsky, I.; Adronov, A. *Chem. Mater.* **2010**, *22*, 2741–2749.
(24) Nish, A.; Hwang, J.; Doig, J.; Nicholas, R. *Nat. Nanotechnol.* **2007**, *2*, 640–646.
(25) Hwang, J.-Y.; Nish, A.; Doig, J.; Douven, S.; Chen, C.-W.; Chen, L.-C.; Nicholas, R. J. *J. Am. Chem. Soc.* **2008**, *130*, 3543–3553.
(26) Campidelli, S.; Ballesteros, B.; Filoramo, A.; Díaz, D. D.; de la Torre, G.; Torres, T.; Rahman, G. M. A.; Ehli, C.; Kiessling, D.; Werner, F.; Sgobba, V.; Guldi, D. M.; Cioffi, C.; Prato, M.; Bourgoin, J.-P. *J. Am. Chem. Soc.* **2008**, *130*, 11503–11509.
(27) Gerard, M.; Chaubey, A.; Malhotra, B. D. *Biosens. Bioelectron.* **2002**, *17*, 345–359.
(28) Xia, L.; Wei, Z.; Wan, M. *J. Colloid Interface Sci.* **2010**, *341*, 1–11.
(29) Ramanavicius, A.; Ramanaviciene, A.; Malinauskas, A. *Electrochim. Acta* **2006**, *51*, 6025–6037.
(30) Borole, D. D.; Kapadi, U. R.; Mahulikar, P. P.; Hundiwale, D. G. *Des. Monomers Polym.* **2006**, *9*, 1–11.
(31) Malhotra, B. D.; Chaubey, A.; Singh, S. P. *Anal. Chim. Acta* **2006**, *578*, 59–74.
(32) Ahuja, T.; Mir, I. A.; Kumar, D.; Rajesh *Biomaterials* **2007**, *28*, 791–805.
(33) Sarma, A. K.; Vatsyayan, P.; Goswami, P.; Minteer, S. D. *Biosens. Bioelectron.* **2009**, *8*, 2313–2322.
(34) Breiby, D. W.; Samuelsen, E. J.; Konovalov, O.; Struth, B. *Langmuir* **2004**, *20*, 4116–4123.
(35) Ogawa, K.; Stafford, J. A.; Rothstein, S. D.; Tallman, D. E.; Rasmussen, S. C. *Synth. Met.* **2005**, *152*, 137–140.
(36) Hiller, M.; Kranz, C.; Huber, J.; Bauerle, P.; Schuhmann, W. *Adv. Mater.* **1996**, *8*, 219–222.
(37) Bunz, U.; Rotello, V. *Angew. Chem., Int. Ed.* **2010**, *49*, 3268–3279.
(38) Wang, J. *Electroanalysis* **2005**, *17*, 7–14.
(39) Ates, M.; Sarac, A. S. *Prog. Org. Coat.* **2009**, *66*, 337–358.
(40) Besteman, K.; Lee, J.-O.; Wiertz, F. G. M.; Heering, H. A.; Dekker, C. *Nano Lett.* **2003**, *3*, 727–730.
(41) Wang, J.; Musameh, M.; Lin, Y. H. *J. Am. Chem. Soc.* **2003**, *125*, 2408–2409.
(42) Tsai, Y.; Li, S.; Chen, J. *Langmuir* **2005**, *21*, 3653–3658.
(43) Holzinger, M.; Haddad, R.; Maaref, A.; Cosnier, S. *J. Nanosci. Nanotechnol.* **2009**, *9*, 6042–6046.
(44) Callegari, A.; Cosnier, S.; Marcaccio, M.; Paolucci, D.; Paolucci, F.; Georgakilas, V.; Tagmatarchis, N.; Vazquez, E.; Prato, M. *J. Mater. Chem.* **2004**, *14*, 807–810.
(45) Xu, L.; Zhu, Y.; Yang, X.; Li, C. *Mater. Sci. Eng., C* **2009**, *29*, 1306–1310.
(46) Chayer, M.; Faid, K.; Leclerc, M. *Chem. Mater.* **1997**, *9*, 2902–2905.
(47) Lukkari, J.; Salomaki, M.; Viinikanoja, A.; Aaritalo, T.; Paukkunen, J.; Kocharova, N.; Kankare, J. *J. Am. Chem. Soc.* **2001**, *123*, 6083–6091.
(48) Trznadel, M.; Zagorska, M.; Lapkowski, M.; Louarn, G.; Lefrant, S.; Pron, A. *Polym. J.* **1996**, *92*, 1387–1393.
(49) Swoboda, B. E. P.; Massey, V. *J. Biol. Chem.* **1965**, *240*, 2209–2215.
(50) Nakamura, S.; Fujiki, S. *J. Biochem.* **1968**, *63*, 51–58.
(51) Shan, D.; Zhang, J.; Xue, H.-G.; Ding, S.-N.; Cosnier, S. *Biosens. Bioelectron.* **2010**, *25*, 1427–1433.
(52) Liu, H.; Hu, N. *Electroanalysis* **2007**, *19*, 884–892.
(53) Zoldák, G.; Zubrik, A.; Musatov, A.; Stupák, M.; Sedlák, E. *J. Biol. Chem.* **2004**, *279*, 47601–47609.
(54) Zhang, S. X.; Wang, N.; Yu, H. J.; Niu, Y. M.; Sun, C. Q. *Bioelectrochemistry* **2005**, *67*, 15–22.
(55) Wilson, R.; Turner, A. P. F. *Biosens. Bioelectron.* **1992**, *7*, 165–185.
(56) Bard, A. J.; Faulkner, L. R. *Electrochemical Methods: Fundamentals and Applications*; 2nd ed.; Wiley: New York, 2001.
(57) Yang, W. W.; Wang, J. X.; Zhao, S.; Sun, Y. Y.; Sun, C. Q. *Electrochem. Commun.* **2006**, *8*, 665–672.
(58) Jeykumari, D. R. S.; Narayanan, S. S. *Carbon* **2009**, *47*, 957–966.
(59) Luo, H. X.; Shi, Z. J.; Li, N. Q.; Gu, Z. N.; Zhuang, Q. K. *Anal. Chem.* **2001**, *73*, 915–920.
(60) Merkoci, A.; Pumera, M.; Llopis, X.; Perez, B.; del Valle, M.; Alegret, S. *TrAC, Trends Anal. Chem.* **2005**, *24*, 826–838.
(61) Wang, J. X.; Li, M. X.; Shi, Z. J.; Li, N. Q.; Gu, Z. N. *Electroanalysis* **2002**, *14*, 225–230.
(62) Liu, J.; Tian, S.; Knoll, W. *Langmuir* **2005**, *21*, 5596–5599.
(63) Zou, Y.; Xiang, C.; Sun, L.-X.; Xu, F. *Biosens. Bioelectron.* **2008**, *23*, 1010–1016.
(64) Wang, H.; Wang, X.; Zhang, X.; Qin, X.; Zhao, Z.; Miao, Z.; Huang, N.; Chen, Q. *Biosens. Bioelectron.* **2009**, *25*, 142–146.
(65) Kamin, R. A.; Wilson, G. S. *Anal. Chem.* **1980**, *52*, 1198–1205.
(66) Shi, Q.; Wang, P.; Jiang, Y.; Kan, J. *Biocatal. Biotransform.* **2009**, *27*, 54–59.
(67) Vidal, J. C.; Garcia, E.; Castillo, J. R. *Biosens. Bioelectron.* **1998**, *13*, 371–382.
(68) Chen, R. J.; Bangsaruntip, S.; Drouvalakis, K. A.; Kam, N. W. S.; Shim, M.; Li, Y. M.; Kim, W.; Utz, P. J.; Dai, H. J. *Proc. Natl. Acad. Sci. U.S.A.* **2003**, *100*, 4984–4989.
(69) Manso, J.; Mena, M. L.; Yanez-Sedeno, P.; Pingarron, J. *J. Electroanal. Chem.* **2007**, *603*, 1–7.